Pion-photon exchange nucleon-nucleon potentials

N. Kaiser

Physik Department T39, Technische Universität München, D-85747 Garching, Germany

In chiral perturbation theory, the dominant next-to-leading-order correction to the $\pi\gamma$-exchange NN-potential proportional to the large isovector magnetic moment $\kappa_v = 4.7$ of the nucleon is calculated. The corresponding spin-spin and tensor potentials $\widetilde{V}_{S,T}(r)$ in coordinate space have a very simple analytical form. At long distances, $r \simeq 2$ fm, these potentials are of similar size (but opposite in sign) as the leading-order $\pi\gamma$-exchange potentials. Effects from virtual Δ-isobar excitation are also considered, as well as other isospin-breaking contributions to the 2π-exchange NN potential induced by additional one-photon exchange.

Isospin violation in the nuclear force is a subject of current interest. Charge-independence breaking (i.e., the difference between the total isospin $I = 1$ *pn* scattering and *nn* or *pp* scattering) is large and well established. On the other hand, charge-symmetry breaking (i.e., the difference between *nn* and *pp* scattering after removal of the long-range electromagnetic forces) is smaller and fairly well established. These isospin-violating contributions to the nuclear force also play an important role in explaining the 764 keV binding-energy difference of ^{3}He and triton [1–3]. The bulk of it, namely 648 keV, can already be understood in terms of the Coulomb interaction [1].

The longest-range isospin-violating NN interaction is generated by the simultaneous exchange of a pion and a photon between the two nucleons. Because the photon is massless, the $\pi\gamma$-exchange interaction is of a nominal one-pion range, $m_\pi^{-1} = 1.41$ fm. After the earlier attempts made in Refs. [4,5], the complete leading-order $\pi\gamma$-exchange NN potential was calculated within the systematic framework of chiral perturbation theory in Ref. [6]. A crucial feature of that calculation was to guarantee the gauge invariance of the result by consideration of the full set of all 19 possible Feynman diagrams. The resulting expression for the complete leading-order $\pi\gamma$-exchange potential in momentum space turned out to be surprisingly simple [see Eq. (1) below]. However, because of its intrinsic smallness (a few permille of the 1π-exchange interaction), the inclusion of this new isospin-breaking interaction had negligible effects on the $^1S_0$ low-energy parameters and it led to only a tiny improvement in the fits of the NN-scattering data [6]. Nevertheless, it is important to know as accurately as possible the size of these well-defined long-range components before one introduces (adjustable) short-range isospin-violating terms.

The purpose of this paper is to calculate next-to-leading-order corrections to the $\pi\gamma$-exchange NN potential within the systematic framework of chiral perturbation theory. These corrections either arise as relativistic $1/M$ corrections (where $M = 939$ MeV is the average nucleon mass) to the static result of Ref. [6] or they are generated by new interaction vertices from the next-to-leading-order chiral Lagrangian $\mathcal{L}_{\pi N}^{(2)}$ [7]. Experience with the isospin-conserving NN potential has shown that the next-to-leading-order corrections are dominated by the contributions proportional to the large low-energy constants,

in that case $c_{1,3,4}$ [8]. For the photon-nucleon coupling, which is of relevance in the present work, one readily identifies the isovector magnetic moment $\kappa_v = 4.7$ of the nucleon as an outstandingly large low-energy parameter. Therefore the focus here is on this particular contribution to the $\pi\gamma$-exchange NN potential. Effects from virtual $\Delta(1232)$-isobar excitation that involve the equally strong $\Delta \to N\gamma$ transition magnetic moment $\kappa^* \simeq 4.9$ are also considered.

Let us start with reanalyzing the leading-order $\pi\gamma$-exchange NN potential of Ref. [6]. The corresponding T matrix in momentum space reads

$$
\begin{aligned}
T_{\pi\gamma}^{(\mathrm{lo})} = {} & \frac{\alpha g_A^2}{8\pi f_\pi^2} \left(\vec{\tau}_1 \cdot \vec{\tau}_2 - \tau_1^3 \tau_2^3 \right) \vec{\sigma}_1 \cdot \vec{q}\, \vec{\sigma}_2 \cdot \vec{q} \\
& \times \left\{ \frac{1}{q^2} - \frac{\left(m_\pi^2 - q^2\right)^2}{q^4\left(m_\pi^2 + q^2\right)} \ln\left(1 + \frac{q^2}{m_\pi^2}\right) \right\},
\end{aligned}
\tag{1}
$$

where $\alpha = 1/137.036$ is the fine-structure constant, $g_A = g_{\pi N} f_\pi / M = 1.3$ is the nucleon axial vector-coupling constant, $f_\pi = 92.4$ MeV is the pion-decay constant, and $m_\pi = 139.57$ MeV is the charged pion mass. Furthermore, $\vec{q}$ denotes the momentum transfer between both nucleons, and $\vec{\sigma}_{1,2}$ and $\vec{\tau}_{1,2}$ are the usual spin and isospin operators of the two nucleons. The Fourier transformation, $-(2\pi)^{-3}\int d^3q \exp(i\vec{q} \cdot \vec{r}), \ldots,$ of Eq. (1) to coordinate space yields a local potential with spin-spin and tensor components:

$$
\begin{aligned}
& \{ \widetilde{V}_S(r)\vec{\sigma}_1 \cdot \vec{\sigma}_2 + \widetilde{V}_T(r)(3\vec{\sigma}_1 \cdot \hat{r}\,\vec{\sigma}_2 \cdot \hat{r} - \vec{\sigma}_1 \cdot \vec{\sigma}_2) \} \\
& \times \tfrac{1}{2}\left(\vec{\tau}_1 \cdot \vec{\tau}_2 - \tau_1^3 \tau_2^3 \right).
\end{aligned}
\tag{2}
$$

The isospin factor $(\vec{\tau}_1 \cdot \vec{\tau}_2 - \tau_1^3 \tau_2^3)/2$ is chosen such that it gives 1 for elastic $pn \to np$ scattering. The leading-order $\pi\gamma$-exchange spin-spin potential reads

$$
\begin{aligned}
\widetilde{V}_S^{(\mathrm{lo})}(r) = {} & \frac{\alpha g_A^2 m_\pi^2}{(4\pi f_\pi)^2} \frac{2e^{-x}}{3r} \left\{ 2\ln\frac{x}{2} + 2\gamma_E - \frac{1}{x} \right. \\
& \left. - \frac{1}{x^2} + \widetilde{E}(x) - 2\widetilde{E}(2x) \right\},
\end{aligned}
\tag{3}
$$

where $x = m_\pi r$. $\widetilde{E}(x) = \int_0^\infty d\zeta\, e^{-\zeta}(\zeta + x)^{-1}$ is the modified exponential integral function, and $\gamma_E \simeq 0.5772$ is the Euler-Mascheroni number. The associated tensor potential has a

TABLE I. Pion-photon exchange pn potentials in units of keV versus the nucleon distance r. The spin-spin and tensor potentials $\widetilde{V}_{S,T}^{(\mathrm{lo})}$ correspond to the leading-order in the chiral expansion. The next-to-leading-order corrections $\widetilde{V}_{S,T}^{(\kappa_v)}$ are proportional to the large isovector magnetic moment $\kappa_v = 4.7$ of the nucleon, and $\widetilde{V}_{S,T}^{(\kappa^*)}$ arise from the magnetic $\Delta \to N\gamma$ transition.

r [fm]	1.0	1.2	1.4	1.6	1.8	2.0	2.2	2.4	2.6	2.8	3.0
$\widetilde{V}_S^{(\mathrm{lo})}$	−52.3	−27.4	−15.0	−8.30	−4.54	−2.35	−1.07	−0.31	0.13	0.37	0.50
$\widetilde{V}_T^{(\mathrm{lo})}$	−48.3	−9.26	3.93	8.06	8.79	8.26	7.31	6.29	5.34	4.49	3.76
$\widetilde{V}_S^{(\kappa_v)}$	61.2	27.7	14.0	7.63	4.41	2.67	1.67	1.08	0.72	0.49	0.34
$\widetilde{V}_T^{(\kappa_v)}$	−230	−100	−49.1	−26.0	−14.6	−8.64	−5.31	−3.37	−2.19	−1.46	−0.99
$\widetilde{V}_S^{(\kappa^*)}$	14.3	5.87	2.70	1.35	0.72	0.41	0.24	0.15	0.09	0.06	0.04
$\widetilde{V}_T^{(\kappa^*)}$	−36.4	−14.3	−6.32	−3.07	−1.60	−0.88	−0.51	−0.30	−0.19	−0.12	−0.08

similar form:

$$
\widetilde{V}_T^{(\mathrm{lo})}(r) = \frac{\alpha g_A^2}{(4\pi f_\pi)^2} \frac{e^{-x}}{3r^3}
$$
$$
\times \left\{ x - 5 + 4(3 + 3x + x^2)\left(\ln\frac{x}{2} + \gamma_E \right) \right.
$$
$$
\left. + (18 - x^2)\widetilde{E}(x) + 4(3x - 3 - x^2)\widetilde{E}(2x) \right\}. \quad (4)
$$

In the first and second rows of Table I some numerical values of these leading-order $\pi\gamma$-exchange potentials are given for distances $1\,\mathrm{fm} \leqslant r \leqslant 3\,\mathrm{fm}$. Somewhat as a surprise, one observes a nonmonotonic dependence on the nucleon distance r. The spin-spin potential $\widetilde{V}_S^{(\mathrm{lo})}(r)$ passes through zero at $r = 2.53$ fm and it has a maximum at $r = 3.34$ fm. For the tensor potential $\widetilde{V}_T^{(\mathrm{lo})}(r)$ these points are shifted inward and reduced by approximately a factor 1.9. It passes through zero at $r = 1.31$ fm and it has its maximum value of about 8.8 keV at $r = 1.78$ fm.

In order to arrive at the analytical results of Eqs. (1), (3), and (4), one can actually circumvent the complete evaluation of all contributing one-loop diagrams. It is sufficient to calculate their spectral function or imaginary part by use of the Cutkosky cutting rule. The pertinent two-body phase-space integral is most conveniently performed in the $\pi\gamma$ center-of-mass frame in which it becomes proportional to a simple angular integral: $(\mu^2 - m_\pi^2)/(32\pi\mu^2) \int_{-1}^{1} dz, \ldots$, where $\mu \geqslant m_\pi$ is the $\pi\gamma$ invariant mass. We can control gauge invariance by working with the (generalized) photon propagator $(-g_{\mu\nu} + \xi k_\mu k_\nu/k^2)/k^2$ through the ξ independence of the total spectral function. Using these techniques, we obtain from the leading-order one-loop $\pi\gamma$-exchange diagrams of Ref. [6]

$$
\mathrm{Im}\, T_{\pi\gamma}^{(\mathrm{lo})} = \frac{\alpha g_A^2}{8 f_\pi^2} (\vec{\tau}_1 \cdot \vec{\tau}_2 - \tau_1^3 \tau_2^3) \, \vec{\sigma}_1 \cdot \vec{q}\, \vec{\sigma}_2 \cdot \vec{q}\, \frac{(\mu^2 + m_\pi^2)^2}{\mu^4 (m_\pi^2 - \mu^2)}. \quad (5)
$$

The notation $\mathrm{Im}\, T_{\pi\gamma}$ is meant here such that one is taking the imaginary part of the amplitude standing to the right of the spin and isospin factors.

Now we turn to the dominant next-to-leading-order correction to the $\pi\gamma$-exchange NN potential proportional to the large isovector magnetic moment $\kappa_v = 4.7$. The relevant

one-loop diagrams with a nucleon in the intermediate state are shown in Fig. 1. The pertinent Feynman rules can be found in Appendix A of Ref. [7]. From the calculated spectral function, $(\mu^2 - m_\pi^2)/\mu^5$ times a polynomial in μ^2 and m_π^2, we derive (by means of a once-subtracted dispersion relation) the following expression for the T matrix in momentum space:

$$
T_{\pi\gamma}^{(\kappa_v)} = \frac{\alpha g_A^2 \kappa_v}{64 M f_\pi^2 q^3} (\vec{\tau}_1 \cdot \vec{\tau}_2 - \tau_1^3 \tau_2^3) \left\{ \vec{\sigma}_1 \cdot \vec{\sigma}_2 \left[(m_\pi^2 + q^2) \right.\right.
$$
$$
\times (3q^2 - m_\pi^2) \arctan\frac{q}{m_\pi} + m_\pi^3 q \right]
$$
$$
+ \frac{1}{q^2} \vec{\sigma}_1 \cdot \vec{q}\, \vec{\sigma}_2 \cdot \vec{q} \left[(m_\pi^2 + q^2)(3m_\pi^2 - 5q^2) \right.
$$
$$
\left. \left. \times \arctan\frac{q}{m_\pi} + 3m_\pi q(q^2 - m_\pi^2) \right] \right\}. \quad (6)
$$

As a side remark, we note that the contribution proportional to the isoscalar magnetic moment $\kappa_s = 0.88$ vanishes identically. The reason for this feature are the vanishing angular integrals: $\fint_{-1}^{1} dz\, z^{-1} = 0 = \int_{-1}^{1} dz\, z$. The Fourier transformation of Eq. (6) to coordinate space yields spin-spin and tensor potentials of the following simple analytical form:

$$
\widetilde{V}_S^{(\kappa_v)}(r) = \frac{\alpha g_A^2 \kappa_v}{48\pi M f_\pi^2} \frac{e^{-m_\pi r}}{r^4} (1 + m_\pi r), \quad (7)
$$

$$
\widetilde{V}_T^{(\kappa_v)}(r) = -\frac{\alpha g_A^2 \kappa_v}{48\pi M f_\pi^2} \frac{e^{-m_\pi r}}{r^4} (5 + 2m_\pi r). \quad (8)
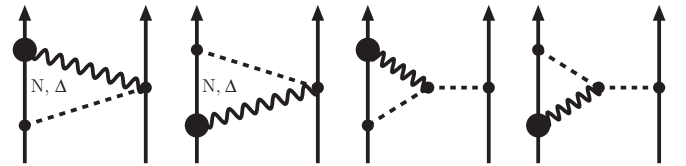$$

FIG. 1. Pion-photon-exchange diagrams generating a nonvanishing imaginary part. The large filled circle symbolizes the magnetic coupling of the photon to the nucleon, or the magnetic $\Delta \to N\gamma$ transition. Diagrams for which the role of both nucleons is interchanged are not shown. These lead effectively to a doubling of the NN potential.

The more direct way to obtain these analytical expressions is to Laplace transform the spectral function Im $T_{\pi\gamma}^{(\kappa_v)}$ [for details see Eqs. (3) and (4) in Ref. [9]]. In the third and fourth rows of Table I some numerical values of these novel isospin-violating potentials $V_{S,T}^{(\kappa_v)}(r)$ are given. At long distances, $r \simeq 2$ fm, they are of the same size but opposite in sign as the leading-order $\pi\gamma$-exchange potentials (compare with the first and second rows in Table I). At shorter distances the tensor component $V_T^{(\kappa_v)}(r)$ in Eq. (8) with its higher weight factor on the singular $1/r^4$ term becomes in fact dominant. Note also that there is some tendency for cancellation in the long-range tails of the tensor potentials.

As argued in Ref. [5], the $\Delta(1232)$ isobar, with its relatively small excitation energy could, also play a substantial role for the $\pi\gamma$-exchange interaction. The transition $\Delta \to N\gamma$ is known to be predominantly of the magnetic dipole type. In the effective chiral Lagrangian approach its strength is parametrized by a transition magnetic moment κ^*. Using empirical information [10] about the partial-decay width,

$$\Gamma(\Delta^+ \to p\gamma) = \frac{\alpha\kappa^{*2}(M_\Delta^2 - M^2)^3}{144 M_\Delta^5 M^2}(3M_\Delta^2 + M^2)$$
$$\simeq 0.68 \, \text{MeV}, \qquad (9)$$

we can extract a value of $\kappa^* \simeq 4.9$ for the $\Delta \to N\gamma$ transition magnetic moment. Here, $M_\Delta = 1232$ MeV denotes the mass of the Δ isobar. The possible one-loop diagrams with virtual excitation of a Δ resonance contributing to the $\pi\gamma$-exchange NN interaction are shown in Fig. 1. The Feynman rules for the nonrelativistic $\pi N\Delta$ and $\gamma N\Delta$ vertices are $(g_{\pi N\Delta}/2M)\vec{S} \cdot \vec{k} \, T^a$ and $(e\kappa^*/2M)\vec{S} \cdot (\vec{k} \times \vec{\epsilon})T^3$, respectively, where $\vec{k}$ denotes an ingoing pion or photon momentum. The 2×4 spin and isospin transition matrices S^i and T^a satisfy the relations $S^i S^{\dagger j} = (2\delta^{ij} - i\epsilon^{ijk}\sigma^k)/3$ and $T^a T^{\dagger b} = (2\delta^{ab} - i\epsilon^{abc}\tau^c)/3$. Using the empirically well-satisfied relation $g_{\pi N\Delta} = 3g_{\pi N}/\sqrt{2} = 3g_A M/\sqrt{2}f_\pi$ for the $\pi N\Delta$ coupling constant, we find the following result for their total spectral function:

$$\text{Im}\,T_{\pi\gamma}^{(\kappa^*)} = \frac{\alpha g_A^2 \kappa^*}{96\sqrt{2}Mf_\pi^2\mu^3}\left(\vec{\tau}_1 \cdot \vec{\tau}_2 - \tau_1^3\tau_2^3\right)$$
$$\times \left\{\vec{\sigma}_1 \cdot \vec{\sigma}_2\left[2\mu\Delta(\mu^2 - m_\pi^2) + (m_\pi^4 + 2m_\pi^2\mu^2\right.\right.$$
$$\left. -3\mu^4 - 4\mu^2\Delta^2)\arctan\frac{\mu^2 - m_\pi^2}{2\mu\Delta}\right]$$
$$+ \vec{\sigma}_1 \cdot \vec{q}\,\vec{\sigma}_2 \cdot \vec{q}\left[2\Delta\left(\frac{m_\pi^2}{\mu} + 3\mu\right)\right.$$
$$+ \left(2m_\pi^2 - 5\mu^2 + \frac{3m_\pi^4}{\mu^2} - \frac{4\Delta^2(3\mu^2 + m_\pi^2)}{\mu^2 - m_\pi^2}\right)$$
$$\left.\left.\times \arctan\frac{\mu^2 - m_\pi^2}{2\mu\Delta}\right]\right\}, \qquad (10)$$

where $\Delta = M_\Delta - M = 293$ MeV denotes the Δ-nucleon mass difference. Note that the spectral function of the spin-spin term (proportional to $\vec{\sigma}_1 \cdot \vec{\sigma}_2$) and the spectral function of the tensor term (proportional to $\vec{\sigma}_1 \cdot \vec{q}\,\vec{\sigma}_2 \cdot \vec{q}$) both vanish at
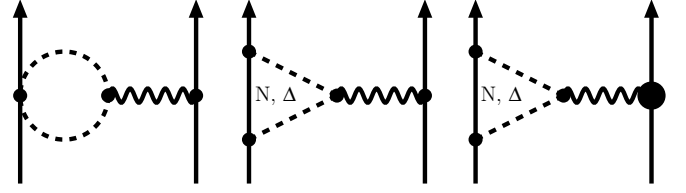

FIG. 2. Isospin-breaking corrections to the two-pion exchange NN interaction induced by one-photon exchange. The large filled circle in the right-hand diagram symbolizes the magnetic coupling of the photon to the nucleon. The 2π-exchange diagrams for which the role of both nucleons is interchanged are not shown.

threshold $\mu = m_\pi$. From the mass spectra given by Eq. (10) one can easily calculate the spin-spin and tensor potentials in coordinate space [following the decomposition in expression (2)] in the form of a continuous superposition of Yukawa functions [9]. The fifth and sixth rows in Table I show the corresponding numerical values for the $\pi\gamma$-exchange potentials $V_{S,T}^{(\kappa^*)}(r)$ for nucleon distances $1 \, \text{fm} \leqslant r \leqslant 3 \, \text{fm}$. One finds that the effects from virtual Δ excitation are about a factor of 5–10 smaller than those generated by diagrams with only nucleon intermediate states. Such a suppression of the Δ-isobar effects has already been speculated on in the summary of Ref. [5]. The present calculation now provides a quantitative answer to this question.

Figure 2 shows another set of isospin-violating contributions to the 2π-exchange NN interaction induced by an additional one-photon exchange. These effects could alternatively be interpreted as one-pion-loop contributions to the electric and magnetic form factors of the nucleon that are introduced in order to describe the electromagnetic interaction between the extended (not pointlike) nucleons. Irrespective of their classification, the magnitude of such isospin-breaking effects should be quantified. The first two diagrams in Fig. 2 (allowing for only an intermediate nucleon state) with the photon coupling to the charge of the nucleon give rise to the following T matrix:

$$T_{\pi\gamma}^{(\text{lo})} = \frac{\alpha}{48\pi f_\pi^2}\left(\tau_1^3 + \tau_2^3 + 2\tau_1^3\tau_2^3\right)$$
$$\times \left[1 + 5g_A^2 + \frac{4m_\pi^2}{q^2}\left(1 + 2g_A^2\right)\right]$$
$$\times \left\{1 - \frac{\sqrt{4m_\pi^2 + q^2}}{q}\ln\frac{q + \sqrt{4m_\pi^2 + q^2}}{2m_\pi}\right\}. \qquad (11)$$

The corresponding central potential in coordinate space,

$$\widetilde{V}_C^{(\text{lo})}(r) = \frac{\alpha}{3(8\pi f_\pi)^2 r}\left(\tau_1^3 + \tau_2^3 + 2\tau_1^3\tau_2^3\right)$$
$$\times \int_{2m_\pi}^\infty d\mu \, e^{-\mu r}\sqrt{\mu^2 - 4m_\pi^2}$$
$$\times \left[\frac{4m_\pi^2}{\mu^2}\left(1 + 2g_A^2\right) - 1 - 5g_A^2\right], \qquad (12)$$

has some similarity with the Uehling potential. As the numbers in the first row of Table II show, it is attractive and of similar size as the leading-order $\pi\gamma$-exchange spin-spin potential (see

TABLE II. Isospin-violating contributions to the two-pion exchange pp potential in units of keV versus the distance r. The spin-spin and tensor potentials $V_{S,T}^{(N,\Delta)}$ are proportional to the large isovector magnetic moment $\kappa_v = 4.7$. The charge-independence-breaking potential $\delta \widetilde{V}_{2\pi}^{(\text{cib})}$ proportional to the pion mass difference $m_{\pi^+} - m_{\pi^0} = 4.59$ MeV is taken from Ref. [11]. The charge-symmetry-breaking potentials $\widetilde{V}_{C,S,T}^{(\text{csb})}$ proportional to the neutron-proton mass difference $M_n - M_p = 1.29$ MeV are taken from Ref. [12].

r [fm]	1.0	1.2	1.4	1.6	1.8	2.0	2.2	2.4	2.6
$\widetilde{V}_C^{(\text{lo})}$	−49.5	−22.5	−11.0	−5.74	−3.13	−1.76	−1.02	−0.61	−0.37
$\widetilde{V}_C^{(\Delta)}$	7.68	2.96	1.26	0.58	0.28	0.14	0.08	0.04	0.02
$\widetilde{V}_S^{(N)}$	−21.3	−8.66	−3.89	−1.88	−0.96	−0.51	−0.28	−0.16	−0.09
$\widetilde{V}_T^{(N)}$	23.9	9.14	3.90	1.81	0.89	0.46	0.25	0.14	0.08
$\widetilde{V}_S^{(\Delta)}$	−4.09	−1.50	−0.62	−0.28	−0.13	−0.07	−0.03	−0.02	−0.01
$\widetilde{V}_T^{(\Delta)}$	4.18	1.46	0.58	0.25	0.12	0.06	0.03	0.02	0.01
$\delta \widetilde{V}_{2\pi}^{(\text{cib})}$	108	55.6	31.1	18.4	11.4	7.25	4.74	3.16	2.14
$\widetilde{V}_C^{(\text{csb})}$	−182	−80.0	−38.9	−20.3	−11.3	−6.51	−3.89	−2.39	−1.50
$\widetilde{V}_S^{(\text{csb})}$	67.3	29.6	14.4	7.50	4.11	2.34	1.38	0.83	0.51
$\widetilde{V}_T^{(\text{csb})}$	−84.1	−34.7	−15.9	−7.86	−4.11	−2.26	−1.28	−0.75	−0.45

the first row in Table I). Here $\widetilde{V}_C^{(\text{lo})}(r)$ has been evaluated for pp scattering, in which the isospin factor $\tau_1^3 + \tau_2^3 + 2\tau_1^3\tau_2^3$ becomes equal to 4. The second diagram in Fig. 2 with a virtual Δ excitation leads to the spectral function:

$$\text{Im}\, T_{\pi\gamma}^{(\Delta)} = \frac{\alpha g_A^2}{8 f_\pi^2 \mu^3}\left(\tau_1^3 + \tau_2^3 + 2\tau_1^3\tau_2^3\right)\Bigg\{\left(\frac{2m_\pi^2}{3} - \Delta^2 - \frac{5\mu^2}{12}\right)$$

$$\times \sqrt{\mu^2 - 4m_\pi^2} + \Delta\left(\mu^2 - 2m_\pi^2 + 2\Delta^2\right)$$

$$\times \arctan \frac{\sqrt{\mu^2 - 4m_\pi^2}}{2\Delta}\Bigg\}. \tag{13}$$

The corresponding central potential $\widetilde{V}_C^{(\Delta)}(r)$ (see second row in Table II) comes out repulsive, and it is approximately an order of magnitude smaller than the leading order one $\widetilde{V}_C^{(\text{lo})}(r)$. The last diagram in Fig. 2 involves the magnetic coupling of the photon to the nucleon. We are considering only the dominant contribution proportional to the isovector magnetic moment $\kappa_v = 4.7$, and we find for the corresponding one-loop T matrix

$$T_{\pi\gamma}^{(N)} = \frac{\alpha g_A^2 \kappa_v}{32 M f_\pi^2}\tau_1^3\tau_2^3 (\vec{\sigma}_1 \times \vec{q}) \cdot (\vec{\sigma}_2 \times \vec{q})$$

$$\times \left\{\frac{2m_\pi}{q^2} - \frac{4m_\pi^2 + q^2}{q^3}\arctan \frac{q}{2m_\pi}\right\}. \tag{14}$$

When translated into coordinate space, spin-spin and tensor potentials are obtained,

$$\widetilde{V}_S^{(N)}(r) = -\frac{\alpha g_A^2 \kappa_v}{96\pi M f_\pi^2}\tau_1^3\tau_2^3 \frac{e^{-2m_\pi r}}{r^4}(1 + 2m_\pi r), \tag{15}$$

$$\widetilde{V}_T^{(N)}(r) = \frac{\alpha g_A^2 \kappa_v}{96\pi M f_\pi^2}\tau_1^3\tau_2^3 \frac{e^{-2m_\pi r}}{r^4}(2 + m_\pi r), \tag{16}$$

of the typical two-pion range $(2m_\pi)^{-1} = 0.7$ fm. As the numbers in the third and fourth row of Table II indicate, they differ from each other mainly in sign. The magnitude of $V_{S,T}^{(N)}(r)$ comes out substantially smaller than that of the central potential $V_C^{(\text{lo})}(r)$. This is to be expected since the magnetic interaction is a higher-order relativistic $1/M$ correction. Finally, a virtual Δ isobar in this two-pion exchange process followed by one-photon exchange is also included. The corresponding spectral function,

$$\text{Im}\, T_{\pi\gamma}^{(\Delta)} = \frac{\alpha g_A^2 \kappa_v}{64 M f_\pi^2 \mu^3}\tau_1^3\tau_2^3 (\vec{\sigma}_1 \cdot \vec{\sigma}_2\, \mu^2 + \vec{\sigma}_1 \cdot \vec{q}\, \vec{\sigma}_2 \cdot \vec{q})$$

$$\times \Bigg\{-2\Delta\sqrt{\mu^2 - 4m_\pi^2} + \left(\mu^2 + 4\Delta^2 - 4m_\pi^2\right)$$

$$\times \arctan \frac{\sqrt{\mu^2 - 4m_\pi^2}}{2\Delta}\Bigg\}, \tag{17}$$

leads to the numerical values of the isospin-violating spin-spin and tensor potentials $V_{S,T}^{(\Delta)}(r)$ presented in the fifth and sixth rows of Table II. These potentials are of the same sign but a factor of 5–10 smaller than their counterparts $V_{S,T}^{(N)}(r)$ with pure nucleon intermediate states.

It is also instructive to compare our present results with previously calculated isospin-breaking 2π-exchange potentials. Taking into account the mass difference between the charged and neutral pion, $m_{\pi^+} - m_{\pi^0} = 4.59$ MeV, in the pion-loops, Friar and van Kolck [11] obtained the charge-independence-breaking central potential $\delta \widetilde{V}_{2\pi}^{(\text{cib})}(r)$ [for an explicit expression, see Eq. (11) in Ref. [11]]. Moreover, the neutron-proton mass difference, $M_n - M_p = 1.29$ MeV, in intermediate nucleon states of the pion loops leads to the charge-symmetry-breaking potentials $\widetilde{V}_{C,S,T}^{(\text{csb})}(r)$ (proportional to $\tau_1^3 + \tau_2^3$) derived recently in Ref. [12] [for details see

Eq. (10) therein]. As one can see from the numerical values in Table II the effects of these hadron mass splittings are substantially larger than the one-photon-exchange correction studies here. For more extensive recent work on isospin-violating NN-forces using the method of unitary transformations, see also Ref. [13].

In summary, in this work next-to-leading-order corrections to the $\pi\gamma$-exchange NN potential were calculated. The dominant contribution proportional to the large isovector magnetic moment $\kappa_v = 4.7$ turns out to be of a similar size (but opposite in sign) as the leading-order term. Effects from virtual Δ-isobar excitation, involving the equally large $\Delta \to N\gamma$ transition magnetic moment $\kappa^* \simeq 4.9$, are approximately one order of magnitude smaller. Furthermore, several isospin-violating contributions to the 2π-exchange NN potential induced by an additional one-photon exchange were also evaluated. In most cases these turned out to be smaller than the $\pi\gamma$-exchange terms and the effects from pion and nucleon mass splittings [11,12]. The analytical expressions for the T matrices and coordinate space potentials derived in this work are in a form that can be easily implemented into NN phase shift analyses or few-body calculations. Such numerical studies will reveal the role of the long-range isospin-violating NN interaction generated by pion-photon exchange.

[1] J. L. Friar, B. F. Gibson, and G. L. Payne, Phys. Rev. C **35**, 1502 (1987).

[2] R. A. Brandenburg *et al.*, Phys. Rev. C **37**, 781 (1988).

[3] Y. Wu, S. Ishikawa, and T. Sasakawa, Phys. Rev. Lett. **64**, 1875 (1990); **66**, 242(E) (1991).

[4] J. S. Leung and Y. Nogami, Nucl. Phys. **B7**, 527 (1968).

[5] J. L. Friar and S. A. Coon, Phys. Rev. C **53**, 588 (1996).

[6] U. van Kolck, M. C. M. Rentmeester, J. L. Friar, T. Goldman, and J. J. de Swart, Phys. Rev. Lett. **80**, 4386 (1998).

[7] V. Bernard, N. Kaiser, and Ulf.-G. Meißner, Int. J. Mod. Phys. E **4**, 193 (1995).

[8] N. Kaiser, R. Brockmann, and W. Weise, Nucl. Phys. **A625**, 758 (1998).

[9] N. Kaiser, Phys. Rev. C **64**, 057001 (2001).

[10] S. Eidelman *et al.* (Particle Data Group), Phys. Lett. **B592**, 1 (2004).

[11] J. L. Friar and U. van Kolck, Phys. Rev. C **60**, 034006 (1999).

[12] J. L. Friar, U. van Kolck, G. L. Payne, and S. A. Coon, Phys. Rev. C **68**, 024003 (2003).

[13] E. Epelbaum and Ulf.-G. Meißner, Phys. Rev. C **72**, 044001 (2005).